

Learning New Tasks from a Few Examples with Soft-Label Prototypes

Avyav Kumar Singh
Department of Informatics
King’s College London

avyav_kumar.singh@kcl.ac.uk

Ekaterina Shutova
ILLC
University of Amsterdam

e.shutova@uva.nl

Helen Yannakoudakis
Department of Informatics
King’s College London

helen.yannakoudakis@kcl.ac.uk

Abstract

Existing approaches to few-shot learning in NLP rely on large language models and fine-tuning of these to generalise on out-of-distribution data. In this work, we propose a simple yet powerful approach to “extreme” few-shot learning, wherein models are exposed to as little as 4 examples per class, based on *soft-label prototypes* that collectively capture the distribution of different classes across the input domain space. Inspired by previous work (Sucholutsky et al., 2021) on univariate or simple multivariate (synthetic) data, we propose a novel approach that is effective on large, high-dimensional and real-world datasets. We learn soft-label prototypes within a neural framework (*DeepSLP*) and we experimentally demonstrate that it achieves superior performance on 31/48 tested tasks and few-shot settings while closely matching the performance of strong baselines on the rest. We focus on learning previously unseen NLP tasks from very few examples (4, 8, 16) and present an in-depth analysis of the effectiveness of our approach.

1 Introduction

Humans have a remarkable ability to adapt knowledge gained in one domain and apply it in another setting, and to identify or disambiguate objects after observing only a handful of examples (Lake et al., 2015). This has inspired research in few-shot learning that aims to build models that can also learn a new task using only a small number of examples per class. Early few-shot learning in NLP relied on interventions at the data level, such as dataset augmentation (Clark et al., 2018) or generation of adversarial examples from few-shot datasets (Miyato et al., 2016). The advent of large language models (LLMs) has now led to a range of approaches, including fine-tuning on

different target tasks (Sun et al., 2020; Zhou and Srikumar, 2022), creating prompt-enhanced few-shot datasets for training (Gao et al., 2020; Schick and Schütze, 2020; Lester et al., 2021), and the application of meta-learning (Finn et al., 2017; Snell et al., 2017) to optimise model parameters such that models adapt quickly to new tasks using past experience (Dou et al., 2019; Holla et al., 2020; van der Heijden et al., 2021) which requires a large number of diverse and balanced few-shot meta-training tasks for effective learning.

In this paper, we propose a simple and effective approach to “extreme” few-shot learning where a model generalises on unseen data after adaptation on as little as 4 examples per class, in the absence of any auxiliary training data and without any LLM finetuning. Inspired by Sucholutsky et al. (2021), we first generate compact representations of input data (by solving for linear constraints) called soft-label prototypes that capture the distribution of different classes across the input domain space, and which are used to make predictions. While the original method of Sucholutsky et al. (2021) is designed for small sets of simple univariate or multivariate (synthetic) data, we extend their approach to work on large sets of high-dimensional and real-world NLP datasets. We then propose a novel method that learns such soft-label prototypes within a neural framework, *DeepSLP*. We focus on learning previously unseen NLP tasks from a few examples per task (4, 8, 16). We experimentally demonstrate that *DeepSLP* outperforms a range of strong few-shot baselines in the majority (31/48) of investigated tasks, while closely matching their performance on the remaining tasks.

2 Related work

Few-shot learning approaches in NLP include data augmentation and semi-supervised learning; e.g., augmentation with adversarial examples (Miyato

et al., 2016), interpolation of training data into a learnable higher dimensional embedding space (Chen et al., 2020), and consistency training to make models more resistant to noise (Xie et al., 2019). Recent research efforts on large-scale pre-training of language models (Devlin et al., 2018; Radford et al., 2019; Brown et al., 2020) reduce the amount of data required for their subsequent fine-tuning in a given task. Instruction tuning (Sanh et al., 2021) and in-context learning (Liu et al., 2021) show that natural language instructions or prompts can enhance a model’s few-shot learning abilities by leveraging the language (instruction) understanding abilities of the given pre-trained LLM. Creating masked language modeling tasks (at training time) with prompts, either in the vocabulary space (Gao et al., 2020) or embedding space (Li and Liang, 2021; Lester et al., 2021), is experimentally demonstrated to give improved performance across classification tasks in few-shot settings compared to LLM fine-tuning for GPT2 (Radford et al., 2019) and BART (Lewis et al., 2019). Sanh et al. (2021) further report that diverse and additional multi-task prompted training leads to better generalisation, less variation on unseen data and an overall superior performance compared to larger state-of-the-art models. However, the search space over LLMs, prompt templates, and few-shot learning is so great that there is yet to be an established standard.

Previous work has also tackled few-shot learning within the meta-learning paradigm of “*learning to learn*”, referring to methods that are trained to adapt quickly (in a few gradient steps) and from a small number of examples using past experience (Finn et al., 2017). Meta-learning has been applied to a range of tasks, including relation extraction and relation classification Obamuyide and Vlachos (2019a,b); word sense disambiguation Holla et al. (2020); sentiment classification, entity-typing and natural language inference Bansal et al. (2020); Nooralahzadeh et al. (2020); part-of-speech tagging (Wang et al., 2020); and dependency parsing (Langedijk et al., 2021).

Despite the many successful applications, however, meta-learning comes with complexities with respect to data and computation (Antoniou et al., 2019). Such methods typically require a large set of diverse and balanced meta-learning tasks for effective learning (Holla et al., 2020), which presents an experimental obstacle to their

widespread use, while training times can span several days as their optimisation is computationally expensive (Bansal et al., 2020).

Our work is more similar to the few-shot learning approach of Bansal et al. (2019), particularly in terms of tasks and datasets used. However, their approach utilises meta-learning together with auxiliary training data (GLUE; Wang et al. (2018)) and it is therefore not directly comparable to ours that focuses on a more realistic (yet more challenging) few-shot learning setting that does not rely on any additional labelled data. To facilitate a comparison, however, we do present an analysis of model performance when such data is available (Section 9.2).

3 Soft-Label Prototypes (SLP)

Sucholutsky and Schonlau (2021) define a soft label as a vector Y representing a data point’s simultaneous membership to several classes. It is used in cases where we can denote a point’s partial association to different classes. Using this definition, they further define a soft-label prototype as (\vec{X}, Y) , where \vec{X} is a point in input space (e.g., an input feature vector) and Y is the corresponding soft label. The underlying idea is that a small set of soft-label prototypes can be used to accurately represent a training set.

3.1 Generating soft-label prototypes

Soft-label prototypes assign soft labels to every point in the input domain; therefore, a soft-label prototype at point \vec{X} represents the class distribution (determined from the training data) at \vec{X} . Based on Algorithm 4 in Sucholutsky et al. (2021), the process of generating soft-label prototypes from training data is a two step process — (1) finding lines that connect the class centroids in the data, where each line connects some of the centroids, and every centroid belongs to one line; and (2) deriving soft-label prototypes capturing the class distribution at the ends of each line.

3.1.1 Finding lines connecting all centroids

The underlying idea here is that we seek to find classes that lie on the same manifold. First, we compute the centroid of each class in the input data. Then, we find and fit class centroids on the minimum number of lines. For this, we use the *recursive regression* method proposed by Sucholutsky et al. (2021). This method clusters centroids hierarchically to group similar (interval) centroids

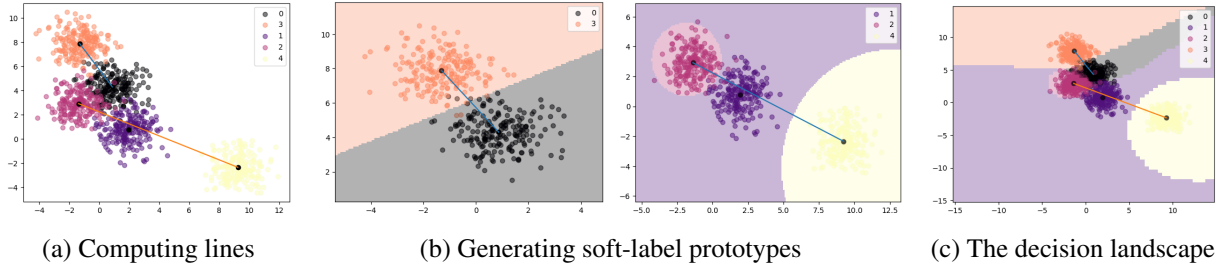


Figure 1: Generating and classifying data with soft-label prototypes.

together, and fits a regression line on the centroids. The similarity of centroids within a single cluster is judged by how well all the centroids fit on a regression line. If the Euclidean distance of a particular centroid is beyond a pre-defined tolerance threshold ϵ from a line, it is removed from that cluster and assigned to another cluster. We use this method for all our experiments, as we experimentally find (on our development data) that it performs well on high-dimensional data spread across many classes such as the ones we test here. In Figure 1(a), we present an example set of lines connecting all centroids. For further details on recursive regression, we refer the reader to Sucholutsky et al. (2021).

3.1.2 Deriving soft-label prototypes by optimising for linear constraints

Once we find the lines, we use the endpoints of each line as the location of soft-label prototypes. Therefore, for l lines fitted on n centroids we have $2l$ prototypes. Sucholutsky et al. (2021) mathematically define finding the class distribution at each end point / soft-label prototype as a constraint optimisation problem. The optimisation problem consists conceptually of two main sets of constraints: (i) the target class at each centroid has the maximum influence amongst all classes at certain points along the line (endpoint of the line and midpoints between classes); and (ii) the difference between the influence of the target class and the sum of the influences of all other classes along the line is maximised. The output of these optimisation constraints are two soft-label prototypes which are “set” at the ends of each line (i.e., \vec{X}) as shown in Figure 1(b). For further details, we refer the reader to Sucholutsky et al. (2021).

3.2 Classification with soft-label prototypes

Given M soft-label prototypes representing the input distribution of N classes, we define $S =$

$(\vec{X}_1, Y_1), \dots, (\vec{X}_M, Y_M)$ to be our set of prototypes, where \vec{X}_i is the location of the i^{th} prototype in the input feature space and Y_i is a matrix of dimension $[N \times 1]$ denoting the soft labels. Given a test datapoint \vec{x} , we find the nearest line to the test point and calculate the Euclidean distances $D = (\vec{X}_i, \vec{x})_{i=1,2,\dots,M}$ from each of the two prototypes of that line to \vec{x} . We then sort S in ascending order of distances using D and weigh the probability distribution of the i^{th} nearest prototype (with a total of two prototypes) inversely by its distance to the point located at \vec{x} to get Y^* :

$$Y^* = \sum_{i=1}^2 \frac{Y_i}{d(\vec{X}_i, \vec{x})} \quad (1)$$

\vec{x} is then assigned the class $C^{SLP}(\vec{x}) = \arg\max_j Y_j^*$ where Y_j^* is the j^{th} element of Y^* . Example decision boundaries using this approach are presented in Figure 1(c). We refer to this method of using soft-label prototypes as *SLP*.

3.3 Classification with SLP: A toy example

Figure 2 presents an example classification with SLP. Given the class centroids for *blue*, *green* and *yellow* are located at $(0, 0)$, $(1.5, 0)$ and $(3, 0)$ respectively, two soft-label prototypes are defined by a line connecting *yellow* and *blue*, and are thus located at $(3, 0)$ and $(0, 0)$ respectively. The soft labels in Figure 2(a) contain the per-class probability distribution derived by the SLP method; for example, $p(x = \text{blue}) = 0.6$ and $p(x = \text{green}) = 0.4$ for the left prototype, and $p(x = \text{green}) = 0.4$ and $p(x = \text{yellow}) = 0.6$ for the right prototype. When a new test instance x located at $(1.5, 0.8)$ is presented, we make predictions as follows: we find the nearest line to x and consider its distance from the two prototypes at the ends of the line and multiply the class distribution of each prototype by the inverse distance as per Eq. 1.

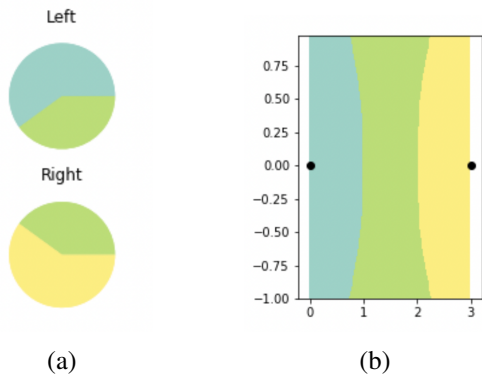


Figure 2: Classification example with SLP (figure from Sucholutsky and Schonlau (2021)).

Since x is equidistant from both prototypes, the distance between the x and each prototype is 1.5. Therefore, the values for *blue* and *yellow* (given both soft-label prototypes) become $\text{soft_label}(x = \text{blue}) = \frac{0.6}{1.5} + \frac{0}{1.5} = 0.4$ and $\text{soft_label}(x = \text{yellow}) = \frac{0}{1.5} + \frac{0.6}{1.5} = 0.4$ respectively. In contrast, for *green*, which is directly informed by both prototypes (i.e., no zero values in the numerator), the probability distribution becomes $\text{soft_label}(x = \text{green}) = \frac{0.4}{1.5} + \frac{0.4}{1.5} = 0.53$. Therefore x is classified as green. This decision boundary can be seen in Figure 2(b).

4 Methodology

We encode training and test instances (Section 5) using base cased BERT (Devlin et al., 2018) from the HuggingFace Transformers¹ library (Wolf et al., 2019). We use the training data to generate soft-label prototypes, and the test data to make predictions as per Eq. 1. We develop and experiment with two variants of the SLP approach, which we describe below. We release our code and models to facilitate further research in the field.

4.1 SLP for NLP data

We use the SLP approach described in Section 3. In order to make SLP powerful enough for large, high-dimensional real-world NLP data (vs univariate, simple multivariate and/or synthetic data), we require an optimiser that scales on such complex data. To this end, we use the MOSEK solver for linear programming (MOSEK ApS, 2019) in the CVXPY library (Diamond and Boyd, 2016) to perform the required computations to generate the

¹<https://huggingface.co/docs/transformers/index>

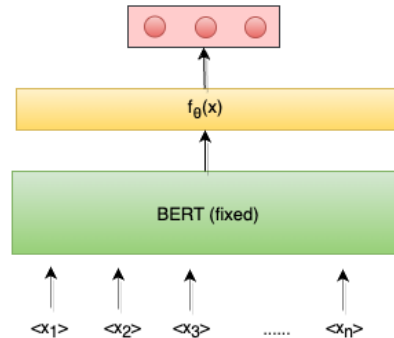


Figure 3: Learning soft-label prototypes (soft labels in red) using a trainable linear layer (yellow): example for a 3-class prototype.

soft-label prototype class distributions.

4.2 DeepSLP: Learning soft labels via gradient descent

We further develop a novel gradient-based approach to generate soft labels as a function of an input x by minimising training loss on a few-shot dataset. After generating lines connecting all class centroids (Section 3.1.1), we set two soft-label prototypes at the ends of the lines. Each soft-label prototype p_i is denoted by $g_{\theta_i}(f(x))$ where g is a neural network parameterised by θ_i and $f(x)$ is a point in the input space. The neural network consists of a fixed encoder (BERT) given by $f(x)$, and a trainable linear layer which returns the soft-label probability distribution at any point x given by $g_{\theta_i}(x)$. Figure 3 presents a visual representation of our approach. Compared to the “standard” SLP variant (Section 4.1) where we find soft-label probability distributions via linear constraint optimisation, we now parameterise our soft-label probability distribution with a neural network.

The trainable linear layer is trained in a few-shot manner (see data setting in Section 5). Crucially, the encoder parameters are frozen as we need our input data points to have an unchanged location in the input space – changing their position might result in class centroids that were previously lying on a straight line to no longer lie on the line. At prediction time, we utilise both soft-label prototypes along the line using Equation 1. A higher distance between a data point x and a prototype leads to a correspondingly smaller effect of the prototype on the final classification; therefore, we want to penalise the prototype that is closer to x

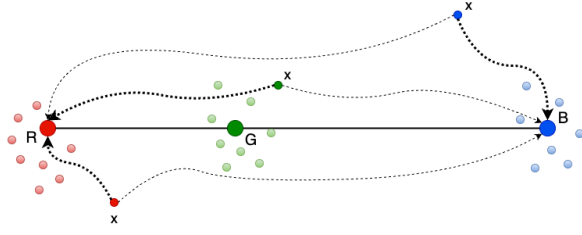


Figure 4: Training soft-label prototypes in DeepSLP. Class centroids are represented with large circles that lie on a line (Red, Green, Blue), while training set examples are represented with smaller circles of the same colour. Dotted lines represent the backpropagation error, of which the bolded ones represent a larger error per soft-label prototype (in case of misclassification). Predictions for x are based on the prototypes at each end of the line.

more if there is an incorrect classification. Each prototype is therefore assigned a fraction of the total loss that is proportional to the other prototype’s Euclidean distance from x . This way, the closer prototype’s weights are corrected more in case of a misclassification. Our approach (DeepSLP) is outlined in Algorithm 1, while an example optimisation is presented in Figure 4.

We use cross entropy loss which gives a measure of the difference between the true and predicted labels. We initialise the weights of $f_{\theta}(x)$ using a uniform Xavier initialisation (Glorot and Bengio, 2010) and use warmup steps to adjust the learning rate. Epochs vary based on the number of classes in the classifier head (between 15 and 25; see datasets used in Section 5): preliminary experiments on the development data show that more epochs are needed when a higher number of classes lie along a line.

5 Tasks and datasets

We use the same tasks and datasets as in Bansal et al. (2019). These cover a variety of text classification tasks with a large number of classes, and include: (a) **Entity typing** – the CoNLL-2003 (Sang and De Meulder, 2003) and MIT-Restaurant (Liu et al., 2013) datasets; (b) **Review rating classification** – review ratings from Amazon Reviews (Blitzer et al., 2007) with a three-way classification; (c) **Text classification** – scraped social me-

Algorithm 1: DeepSLP

```

1  $\lambda \leftarrow$  set of lines connecting all centroids
2  $f_{\theta_l}$  is the network parameterised by  $\theta_l$  for
   the left-end prototype on a line
3  $f_{\theta_r}$  is the network parameterised by  $\theta_r$  for
   the right-end prototype on a line
4  $\mathcal{J} \leftarrow$  loss function
5  $D \leftarrow$  training data
6 Require  $\lambda \neq \emptyset$ 
7 for  $i \in \lambda$  do
8   for  $epoch$  1..... $N$  do
9      $p_{il} \leftarrow$  location of left prototype
10     $p_{ir} \leftarrow$  location of right prototype
11    for  $x \in minibatch(D)$  do
12       $d_1 \leftarrow \|p_{il} - x\|$ 
13       $d_2 \leftarrow \|p_{ir} - x\|$ 
14       $pred.append\left(\frac{f_{\theta_{il}}(x)}{d_1} + \frac{f_{\theta_{ir}}(x)}{d_2}\right)$ 
15    end
16     $d\_loss \leftarrow \mathcal{J}(pred, D)$ 
17     $loss_1 \leftarrow \frac{d_2}{d_1+d_2} * d\_loss$ 
18     $loss_2 \leftarrow \frac{d_1}{d_1+d_2} * d\_loss$ 
19     $\theta_{il} \leftarrow \theta_{il} - \eta \nabla_{\theta_{il}} loss_1$ 
20     $\theta_{ir} \leftarrow \theta_{ir} - \eta \nabla_{\theta_{ir}} loss_2$ 
21  end
22 end

```

dia data from crowdflower² comprising sentiment and emotion classification in a range of domains, as well as political bias detection; and (d) **Natural language inference** in the scientific domain – the SciTail dataset (Khot et al., 2018). We randomly sample 1000 instances from the emotion task in (c) and use them as our held-out validation set for hyperparameter tuning.

We use the same data splits as Bansal et al. (2019), which are publicly available.³ At evaluation time, Bansal et al. (2019) sample an N -way k -shot training (support set) subset $\forall k \in \{4, 8, 16\}$ for few-shot fine-tuning and then evaluate model performance on the test set of each respective task. As performance is dependent on the data used for fine-tuning, they sample 10 different subsets per task, and report the averaged performance across subsets on the test set. We utilise the same subsets as Bansal et al. (2019) for fine-tuning our models too. Unlike Bansal et al. (2019), however, we do

²<https://www.figure-eight.com/data-for-everyone/>

³<https://github.com/iesl/leopard/>

not utilise auxiliary training data (GLUE; Wang et al. (2018)), and only train our models on the few-shot training subsets provided. This makes our setting more challenging but one which is testing a more realistic few-shot setting that does not rely on additional data and labels. While we are not directly comparable to Bansal et al. (2019), to facilitate such a comparison, we present an analysis where we also utilise GLUE data (Section 9.2).

Similar to Bansal et al. (2019), we use mean accuracy and standard deviation to evaluate performance. For entity typing tasks, we obtain token-level encodings for classification.

6 Baselines

Our aim is to determine how well our soft-label prototype models perform compared to other classifiers given the same few-shot training data. Again, our focus is on performing an extreme few-shot learning scenario where no auxiliary data is available, and so we choose such baseline comparisons accordingly.

1-Nearest Neighbour Classifier Our first baseline is a 1-Nearest Neighbour classifier for each task. This is motivated by the fact that test time predictions using soft-label prototypes depend on the soft-label functions of the closest class centroids to a test point x (Section 3.2). We first encode all data points using BERT, and then assign test instances the class of their closest training example in this embedding space based on Euclidean distance.

Fine-tuned BERT We use the BERT baseline reported in Bansal et al. (2019), which is fine-tuned (all layers) on the training set of each task and is trained using the same experimental/few-shot setting as ours. We refer to this model as $\text{BERT}_{\text{fine-tuned}}$.

Prototypical Networks We use Prototypical networks (ProtoNets) (Snell et al., 2017) as another baseline to evaluate generalisation within a few-shot meta-learning setup. ProtoNet is a metric-based meta-learning method that uses an embedding function f_θ to encode training samples and compute a high-dimensional vector μ_c that is the arithmetic mean of the training data points of class c . It then uses a distance function d to compute the similarity between a test instance x and the mean vector of each class, and get the class

probability distribution as:

$$p(y = c|x) = \text{softmax}(-d(f_\theta(x), \mu_c)) \\ = \frac{\exp(-d(f_\theta(x), \mu_c))}{\sum_{c' \in C} \exp(-d(f_\theta(x), \mu_{c'}))}$$

The model is optimised using negative log-likelihood. We use BERT as the encoder and fine-tune it (all layers) using our few-shot training sets and a learning rate of $3e-5$.

7 Experimental setup

Generating lines The hyperparameters used to generate lines are: (a) ϵ , which is a control factor used to denote the maximum tolerance between a centroid and the line assigned to it using Euclidean distance—we use a tolerance value of $1e-1$; and (b) l , which denotes the maximum number of lines used to connect all centroids. We experiment with a range of values ($l \in \{0.25n, 0.5n, 0.75n, n-1\}$, where n is the number of centroids), but find $l = \lceil n/2 \rceil$ to give the best accuracy on the validation data with the minimum number of lines required.⁴

DeepSLP For DeepSLP, we find that more epochs are needed to train models with a higher number of soft labels (i.e., a higher number of classes in the output of the classifier head). In other words, 3 classes fitted on a line need more epochs compared to 2 classes fitted on a line. We use *AdamW* (Loshchilov and Hutter, 2017) as our optimiser and perform hyperparameter tuning on the validation set. We find we only need a few epochs to generalise well – these range from 5 to 10 depending on the training task. We evaluate our approach and all baselines in the following manner: we fix a random seed, train our models, and evaluate performance on the test tasks. We repeat this process across three different seeds, and report the mean and standard deviation at test time.

8 Results and discussion

Our results (Table 1) demonstrate that $\text{DeepSLP}_{\text{BERT}}$ outperforms $\text{BERT}_{\text{fine-tuned}}$ in 31/48 tasks, SLP_{BERT} in 43/48 tasks and 1-NN in 41/48 tasks, demonstrating the usefulness of soft-label prototypes and superiority over the “standard” LLM fine-tuning paradigm, as well as the simpler SLP variant. SLP_{BERT} , on the other

⁴The right choice of hyperparameters is key as the optimisation process fails when it is not possible to connect n centroids with l lines.

Category (Classes)	Shot	INN	ProtoNet	BERT _{fine-tuned} *	SLP _{BERT}	DeepSLP _{BERT}
Rating DVD (3)	4	38.289 ± 6.846	37.665 ± 7.184	32.22 ± 08.72	32.298 ± 16.263	39.566 ± 5.086
	8	37.598 ± 5.364	37.008 ± 5.118	36.35 ± 12.50	32.644 ± 16.016	38.788 ± 4.449
	16	37.461 ± 4.506	39.123 ± 6.004	42.79 ± 10.18	35.587 ± 17.445	40.53 ± 4.375
Rating Electronics (3)	4	37.001 ± 5.164	33.696 ± 5.55	39.27 ± 10.15	35.188 ± 16.211	39.977 ± 5.959
	8	37.646 ± 4.223	37.297 ± 5.938	28.74 ± 08.22	29.624 ± 12.876	41.926 ± 3.985
	16	38.633 ± 3.103	43.825 ± 5.946	45.48 ± 06.13	29.836 ± 12.753	44.917 ± 3.164
Political Bias (2)	4	52.245 ± 4.348	51.15 ± 2.454	54.57 ± 5.02	53.447 ± 3.281	53.251 ± 4.042
	8	54.568 ± 3.015	56.568 ± 4.228	56.15 ± 3.75	55.824 ± 3.725	58.209 ± 5.198
	16	55.884 ± 2.436	59.183 ± 4.706	60.96 ± 4.25	58.277 ± 4.128	61.479 ± 2.974
Rating Kitchen (3)	4	36.769 ± 7.738	35.914 ± 6.678	34.76 ± 11.20	28.253 ± 15.907	39.624 ± 6.787
	8	37.435 ± 6.347	38.46 ± 11.124	34.49 ± 08.72	24.397 ± 11.961	41.081 ± 6.777
	16	38.047 ± 3.226	46.546 ± 8.394	47.94 ± 08.28	31.926 ± 18.29	45.801 ± 4.562
Political Audience (2)	4	51.827 ± 1.754	50.976 ± 1.84	51.02 ± 1.72	51.305 ± 2.68	51.741 ± 2.827
	8	53.113 ± 2.314	52.022 ± 3.964	52.80 ± 2.72	53.104 ± 3.669	54.506 ± 3.274
	16	53.287 ± 1.874	54.024 ± 3.071	58.45 ± 4.98	53.888 ± 3.305	56.956 ± 3.045
Sentiment Kitchen (2)	4	60.17 ± 3.197	55.24 ± 3.427	56.93 ± 7.10	61.96 ± 4.594	60.76 ± 4.426
	8	59.82 ± 2.703	62.28 ± 5.103	57.13 ± 6.60	64.83 ± 3.983	65.733 ± 3.198
	16	61.85 ± 2.65	66.9 ± 5.441	68.88 ± 3.39	68.21 ± 3.298	69.18 ± 2.589
Disaster (2)	4	53.629 ± 9.391	51.474 ± 8.848	55.73 ± 10.29	52.77 ± 10.803	54.252 ± 9.843
	8	57.625 ± 7.638	60.661 ± 4.991	56.31 ± 09.57	56.888 ± 11.139	61.3 ± 7.961
	16	60.93 ± 4.997	63.893 ± 6.62	64.52 ± 08.93	65.907 ± 3.691	69.28 ± 2.358
Airline (3)	4	46.175 ± 4.922	44.167 ± 10.752	42.76 ± 13.50	36.243 ± 22.607	50.987 ± 4.936
	8	48.039 ± 5.677	50.148 ± 13.429	38.00 ± 17.06	44.972 ± 22.584	55.209 ± 6.049
	16	51.754 ± 2.954	54.8 ± 10.49	58.01 ± 08.23	29.238 ± 17.494	60.247 ± 4.577
Emotion (13)	4	8.474 ± 1.028	8.953 ± 2.052	09.20 ± 3.22	8.662 ± 6.213	9.706 ± 1.108
	8	8.418 ± 0.792	10.857 ± 3.436	08.21 ± 2.12	8.16 ± 3.266	8.041 ± 2.797
	16	8.758 ± 0.854	11.479 ± 2.96	13.43 ± 2.51	8.115 ± 3.66	10.919 ± 1.615
Rating Books (3)	4	39.324 ± 4.985	37.715 ± 5.801	39.42 ± 07.22	25.562 ± 15.207	42.116 ± 4.725
	8	38.447 ± 4.07	38.518 ± 5.327	39.55 ± 10.01	34.026 ± 14.123	42.156 ± 4.608
	16	41.107 ± 2.683	44.694 ± 7.797	43.08 ± 11.78	32.509 ± 16.132	46.513 ± 3.036
Political Message (9)	4	15.044 ± 1.556	13.888 ± 2.076	15.64 ± 2.73	12.438 ± 1.799	14.421 ± 1.095
	8	15.666 ± 1.053	16.155 ± 2.316	13.38 ± 1.74	15.08 ± 2.925	16.919 ± 1.756
	16	14.844 ± 1.426	18.324 ± 2.011	20.67 ± 3.89	13.121 ± 3.294	18.319 ± 1.74
Scitail (2)	4	53.66 ± 4.594	50.227 ± 5.69	58.53 ± 09.74	52.296 ± 4.366	54.101 ± 3.759
	8	53.212 ± 3.028	54.196 ± 6.678	57.93 ± 10.70	55.964 ± 5.705	56.341 ± 5.786
	16	54.53 ± 4.399	57.744 ± 5.696	65.66 ± 06.82	59.675 ± 4.033	59.692 ± 4.227
Sentiment DVD (2)	4	53.78 ± 1.316	51.06 ± 3.302	54.98 ± 3.96	56.06 ± 2.408	55.003 ± 2.936
	8	53.8 ± 2.843	55.19 ± 3.298	55.63 ± 4.34	56.98 ± 3.299	57.527 ± 3.562
	16	54.05 ± 1.659	59.45 ± 3.84	58.69 ± 6.08	58.95 ± 2.813	60.76 ± 2.944
Sentiment Books (2)	4	57.56 ± 4.571	55.53 ± 4.097	54.81 ± 3.75	59.89 ± 5.385	58.67 ± 4.753
	8	60.76 ± 4.177	58.97 ± 4.909	53.54 ± 5.17	64.34 ± 2.565	64.78 ± 2.615
	16	60.98 ± 2.857	65.5 ± 7.026	65.56 ± 4.12	66.36 ± 2.183	67.453 ± 3.085
Restaurant (8)	4	48.194 ± 4.881	18.161 ± 2.822	49.37 ± 4.28	24.932 ± 17.102	47.634 ± 5.237
	8	57.36 ± 3.681	32.146 ± 5.785	49.38 ± 7.76	29.787 ± 9.573	55.912 ± 4.494
	16	64.706 ± 2.913	40.435 ± 3.348	69.24 ± 3.68	29.154 ± 13.537	61.716 ± 2.208
CoNLL (4)	4	45.104 ± 7.724	35.438 ± 7.324	50.44 ± 08.57	27.02 ± 7.346	52.724 ± 5.84
	8	46.897 ± 4.183	44.259 ± 4.886	50.06 ± 11.30	31.296 ± 17.487	60.374 ± 3.731
	16	53.969 ± 3.252	52.116 ± 5.354	74.47 ± 03.10	22.923 ± 7.933	67.496 ± 4.551

Table 1: Classification performance (accuracy) of our methods (SLP and DeepSLP) and baselines. Entries in green indicate the best model; * is the baseline as reported in Bansal et al. (2019). Subscripts for SLP and DeepSLP refer to the (non-fine-tuned) encoder used.

#	SLP	DeepSLP
1	$5.6422e - 01$	$9.7887e - 01$
	$4.3577e - 01$	$1.3500e - 04$
	$9.7973e - 16$	$2.0995e - 02$
2	$5.3090e - 13$	$2.5240e - 02$
	$4.3212e - 01$	$1.0000e - 05$
	$5.6787e - 01$	$9.7475e - 01$

Table 2: Soft labels derived from SLP and DeepSLP. # denotes the index of the soft-label prototype lying on the line.

hand, fares worse than $BERT_{\text{fine-tuned}}$ and 1-NN, outperforming the former in only 19/48 tasks and the latter in 17/48 tasks, while exhibiting high standard deviations. Overall, DeepSLP is the best performing method, demonstrating the highest accuracy in 31/48 tasks, while being on-par with the second best model ($BERT_{\text{fine-tuned}}$) on the remaining tasks (15/48 tasks).

SLP vs. DeepSLP From Table 1, we can see that SLP exhibits high standard deviations, in particular for tasks with a high number of classes ($N > 2$).⁵ SLP’s behaviour can be explained by the fact that it can, at times, fail to select the nearest centroid (proof provided in Theorem 12.1), as demonstrated in the example in Figure 5. If we consider the case where $N = 2$, then SLP essentially acts as a 1-NN with soft labels trivially at $[1, 0]$ and $[0, 1]$, with class centroids acting as the nearest neighbour. However, when generalising beyond this setting, the model’s stability is affected. SLP optimises soft labels using the geometric properties of a line and does not consider each (training) data point individually – the soft labels produced by SLP are constants. DeepSLP, on the other hand, learns from training data and produces soft labels as a function of an input point; therefore, it has the ability to output soft labels based on the location of an input (test) point (with the location of the prototypes being fixed).

In Table 2, we further present the probability distribution of two soft-label prototypes for the category Airline using SLP and DeepSLP with the

⁵The only exceptions to this are Disaster ($N = 2$), where we observe a high standard deviation across all models; and Emotion ($N = 13$) and Political Message ($N = 9$), where we observe lower standard deviations. There we only find lines containing 2 centroids (except for one with 3 centroids). This low number of classes per line is therefore responsible for the higher stability and, in turn, lower standard deviations.

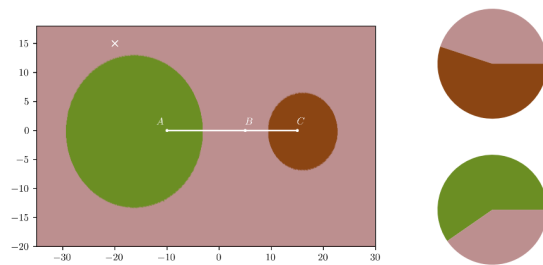


Figure 5: The centroids for classes A (green), B (pink) and C (red) are located at $(-12, 0)$, $(5, 0)$ and $(15, 0)$ respectively. Unlike most Euclidean distance based algorithms such as 1-NN, the test point marked by x is assigned to B (instead of the nearest class, A) with SLP. The soft labels at $(-15, 0)$ and $(15, 0)$ are represented in the pie charts on the right.

16-shot setting. It can be seen that the distribution of soft labels derived from SLP tends to be more skewed, with the probability distribution lying heavily on 2/3 classes, which is in contrast to DeepSLP that seems to be more uniform. This is a pattern that we generally observe across all tasks. This can further explain the lower performance of SLP, as this behaviour essentially tends to dismiss an entire class. DeepSLP, on the other hand, leads to better generalisation and a more stable performance in our highly limited data setting.

Number of shots For DeepSLP, we observe a general trend where performance increases as the number of shots increases from 4 to 16. On the other hand, for SLP, we do not see as clear a picture, indicating that more data does not necessarily improve performance (e.g., there is a decrease in performance for SLP in 7/16 test tasks as we move from 8 to 16 shots).

(Deep)SLP training time and model parameters Training time reduces to three operations: encoding the data, generating lines from class centroids, and constructing soft-label prototypes at the ends of the lines. Generally, we observe that (a) all lines are constructed under a second, (b) soft labels via optimisation of linear constraints using the MOSEK solver are generated in less than a second, and (c) soft labels learned by minimising training loss require less than 10 seconds per line (tasks with $N = 2$ or $N = 3$ use only one line, except for emotion which has $N = 13$ and takes less than a minute). Furthermore, the num-

ber of parameters are substantially smaller compared to those in fine-tuning an LLM – we only need to fine-tune 1500 – 10000 parameters (based on the number of classes) for the linear layer of each soft-label prototype for DeepSLP, compared to $> 10^8$ parameters for finetuning BERT. DeepSLP does not require a GPU.

9 Further analysis

9.1 DeepSLP architecture analysis

There are three properties of DeepSLP that contribute to its performance: the location of the prototypes, the distance metrics, and the learnable soft labels. The first two are intertwined and inherited from SLP (and tested using the SLP baseline above), while the last is unique to DeepSLP and results in dynamically generated soft labels that are superior compared to the the fixed SLP ones. In this section, we seek to further quantify the effectiveness of DeepSLP by now comparing it against a simpler counterpart that only utilises the architecture of DeepSLP, that is, fixed BERT followed by a trainable linear layer (ensuring we keep the seeds fixed across models), which we refer to as simply BERT. As the seeds of both models are fixed, we are able to eliminate any randomness in the test setting and thus have a clear contrast between the performance of the two methods. In Table 3, we observe that DeepSLP is indeed superior to BERT. The difference between the two tends to reduce as k increases, which highlights the usefulness of DeepSLP in extreme few-shot settings. Interestingly, we also observe that BERT outperforms $\text{BERT}_{\text{fine-tuned}}$ in 12/48 tasks (Table 1).

9.2 Using a more powerful encoder

While our focus is on extreme few-shot learning utilising limited amounts of training data, in this section, we seek to analyse model behaviour when auxiliary labelled data is available. Specifically, we utilise another encoder, MT-DNN (Liu et al., 2019), a BERT model that has been fine-tuned on the GLUE (Wang et al., 2018) dataset (similarly to Bansal et al. (2019)), and which we further fine-tune on our data, similarly to our fine-tuned BERT baseline. In Table 4, we present the performance of MT-DNN (fine-tuned) and a DeepSLP variant that uses the MT-DNN encoder (fixed). We can see that the performance of the two is closer in this case (compared to when using the BERT encoder in Table 1) – DeepSLP outperforms MT-DNN in

Category (Classes)	Shot	BERT	DeepSLP _{BERT}
Rating DVD (3)	4	36.142 ± 8.17	39.566 ± 5.086
	8	37.855 ± 5.208	38.788 ± 4.449
	16	41.465 ± 4.597	40.53 ± 4.375
Rating Electronics (3)	4	37.815 ± 9.3	39.977 ± 5.959
	8	40.901 ± 3.97	41.926 ± 3.985
	16	45.289 ± 2.832	44.917 ± 3.164
Political Bias (2)	4	52.466 ± 2.776	53.251 ± 4.042
	8	57.819 ± 4.709	58.209 ± 5.198
	16	61.025 ± 2.879	61.479 ± 2.974
Rating Kitchen (3)	4	38.954 ± 12.067	39.624 ± 6.787
	8	40.511 ± 8.019	41.081 ± 6.777
	16	44.923 ± 3.536	45.801 ± 4.562
Political Audience (2)	4	51.069 ± 1.259	51.741 ± 2.827
	8	54.117 ± 2.824	54.506 ± 3.274
	16	56.827 ± 3.438	56.956 ± 3.045
Sentiment Kitchen (2)	4	58.697 ± 4.943	60.76 ± 4.426
	8	63.473 ± 3.207	65.733 ± 3.198
	16	69.14 ± 2.413	69.18 ± 2.589
Disaster (2)	4	54.005 ± 10.75	54.252 ± 9.843
	8	61.644 ± 6.371	61.3 ± 7.961
	16	68.378 ± 2.686	69.28 ± 2.358
Airline (3)	4	44.714 ± 14.082	50.987 ± 4.936
	8	53.887 ± 7.074	55.209 ± 6.049
	16	59.967 ± 3.842	60.247 ± 4.577
Emotion (13)	4	10.068 ± 2.714	9.706 ± 1.108
	8	11.876 ± 0.743	8.041 ± 2.797
	16	12.124 ± 1.945	10.919 ± 1.615
Rating Books (3)	4	40.832 ± 8.488	42.116 ± 4.725
	8	41.842 ± 5.425	42.156 ± 4.608
	16	46.494 ± 2.465	46.513 ± 3.036
Political Message (9)	4	15.311 ± 2.265	14.421 ± 1.095
	8	18.244 ± 1.636	16.919 ± 1.756
	16	18.971 ± 2.206	18.319 ± 1.74
Scitail (2)	4	51.474 ± 6.275	54.101 ± 3.759
	8	55.173 ± 6.254	56.341 ± 5.786
	16	59.887 ± 3.667	59.692 ± 4.227
Sentiment DVD (2)	4	54.457 ± 2.97	55.003 ± 2.936
	8	56.54 ± 4.009	57.527 ± 3.562
	16	60.593 ± 2.73	60.76 ± 2.944
Sentiment Books (2)	4	57.217 ± 3.822	58.67 ± 4.753
	8	63.87 ± 3.982	64.78 ± 2.615
	16	67.137 ± 3.107	67.453 ± 3.085
Restaurant (8)	4	25.63 ± 3.834	47.634 ± 5.237
	8	37.475 ± 2.683	55.912 ± 4.494
	16	44.132 ± 3.33	61.716 ± 2.208
CoNLL (4)	4	47.97 ± 5.926	52.724 ± 5.84
	8	62.647 ± 4.582	60.374 ± 3.731
	16	70.314 ± 2.23	67.496 ± 4.551

Table 3: Contrasting the performance of DeepSLP to a counterpart (BERT) that only tests the architecture of DeepSLP.

23/48 tasks, but the differences are small ($< 1\%$ in 18/48 tasks, with similar standard deviation). Again, this highlights DeepSLP’s effectiveness in data lean settings. Furthermore, DeepSLP does not require a GPU while only trains a fraction of the parameters used in MT-DNN finetuning.

10 Ensemble properties of DeepSLP

In this study, we compare and contrast DeepSLP to ensembles and draw similarities between the two, shedding further light into the effectiveness of our approach. Each prediction decision by DeepSLP is the result of two soft-label prototypes

Category (Classes)	Shot	MT-DNN	DeepSLP _{MT-DNN}
Rating DVD (3)	4	51.26 ± 8.3	57.87 ± 7.3
	8	55.39 ± 10.07	53.96 ± 5.68
	16	60.02 ± 1.8	56.2 ± 6.43
Rating Electronics (3)	4	59.82 ± 4.24	57.63 ± 7.91
	8	63.37 ± 0.78	60.51 ± 2.91
	16	62.85 ± 0.62	61.47 ± 2
Political Bias (2)	4	62.46 ± 4.09	61.25 ± 9.25
	8	66.37 ± 0.36	63.83 ± 4.53
	16	66.10 ± 3.79	65.63 ± 2.03
Rating Kitchen (3)	4	54.80 ± 13.02	56.81 ± 13.42
	8	57.08 ± 11.95	57.47 ± 9.99
	16	63.95 ± 4.34	62.02 ± 4.83
Political Audience (2)	4	51.03 ± 7.22	52.87 ± 7.28
	8	56.74 ± 5.30	56.78 ± 3.72
	16	58.70 ± 2.15	58.78 ± 2.83
Sentiment Kitchen (2)	4	82.50 ± 3.49	86.65 ± 0.54
	8	86.67 ± 0.60	86.09 ± 1.26
	16	86.63 ± 0.50	86.87 ± 0.26
Disaster (2)	4	50.29 ± 3.60	51.28 ± 3.44
	8	51.61 ± 5.07	56.67 ± 5.29
	16	56.08 ± 4.77	53.23 ± 1.94
Airline (3)	4	70.41 ± 2.45	63.65 ± 11.7
	8	70.22 ± 2.47	70.8 ± 2.69
	16	71.04 ± 0.64	72.51 ± 1.14
Emotion (13)	4	12.88 ± 0.73	10.39 ± 2.71
	8	15.39 ± 1.37	11.17 ± 2.16
	16	17.45 ± 0.56	11.24 ± 1.99
Rating Books (3)	4	65.52 ± 8.96	62.25 ± 6.79
	8	69.28 ± 0.27	63.27 ± 3.16
	16	68.94 ± 0.78	68.02 ± 1.8
Political Message (9)	4	19.78 ± 1.10	18.38 ± 2.13
	8	21.56 ± 0.65	21.16 ± 1.72
	16	23.63 ± 2.47	23.02 ± 1.11
Scitail (2)	4	56.11 ± 3.52	63.71 ± 6.85
	8	69.36 ± 3.41	73.33 ± 5.63
	16	74.18 ± 3.38	73.81 ± 3.66
Sentiment DVD (2)	4	84.30 ± 0.96	84.57 ± 1.05
	8	84.90 ± 0.75	84.18 ± 1.41
	16	84.73 ± 0.52	85.09 ± 0.28
Sentiment Books (2)	4	85.53 ± 0.99	86.23 ± 0.4
	8	85.43 ± 0.34	85.6 ± 1.23
	16	85.73 ± 0.71	86.18 ± 0.33
Restaurant (8)	4	28.37 ± 2.65	34.28 ± 5.23
	8	46.65 ± 3.80	44.15 ± 5.43
	16	58.66 ± 1.24	47.09 ± 3.71
CoNLL (4)	4	35.97 ± 2.38	47.33 ± 6.2
	8	49.04 ± 0.63	59.13 ± 5.14
	16	64.55 ± 1.14	61.96 ± 5

Table 4: Contrasting the performance of DeepSLP to MT-DNN.

– those that lie on each end of the line nearest to a test point x . An analogy can then be drawn between the prototypes used at prediction time and those individual (albeit independent) models that are utilised by an ensemble when producing the final classification. While DeepSLP prototypes are not independent but are rather trained jointly (and share the same encoder), in what follows, we demonstrate that they display several properties of ensemble methods, while being computationally efficient and utilising a small number of parameters. For the analyses below, we consider the tasks Airline and Disaster using an 8-shot setting and evaluate on the test data for each.

10.1 Individual vs joint prediction

In a similar way as an ensemble exhibits superior performance to the individual models it utilises, we seek to assess whether the joint utilisation of prototypes at prediction time is indeed more effective than utilising each prototype individually. To evaluate this, we measure the probability distribution of each setting on the test data using negative log-likelihood:

$$NLL(\mathbf{f}(\mathbf{x}), y) \triangleq -\log(\mathbf{f}^{(y)}(\mathbf{x}))$$

Following Abe et al. (2022), for a strictly convex function such as NLL , we use Jensen’s inequality:

$$NLL(\mathbf{F}(\mathbf{x}), y) \leq \mathbb{E}[NLL(\mathbf{f}(\mathbf{x}), y)]$$

where $\mathbf{F}(\mathbf{x})$ is the ensemble and $\mathbf{f}(\mathbf{x})$ are the constituent models. The idea is that the probability distribution of the ensemble fits the target distribution more closely than the corresponding expected probability distributions of its constituent models. For joint soft-label prototypes parameterised by g_1 and g_2 and located at p_1 and p_2 , we have:

$$\begin{aligned} NLL \left(\text{softmax} \left(\frac{g_1(f(x))}{\|f(x) - p_1\|} + \frac{g_2(f(x))}{\|f(x) - p_2\|} \right), y \right) \\ = - \sum \log \left(\text{softmax} \left(\frac{g_1^y(f(x))}{\|f(x) - p_1\|} + \frac{g_2^y(f(x))}{\|f(x) - p_2\|} \right) \right) \end{aligned}$$

For the individual soft-label prototypes, weighing the outputs by distance does not change the final softmax probability distribution; therefore, we can define $\mathbb{E}[NLL(\mathbf{f}(\mathbf{x}), y)]$ as their average:

$$-\frac{1}{2} \sum \log(\text{softmax}(g_1^y(f(x))) + \log(\text{softmax}(g_2^y(f(x))))$$

We plot the negative log likelihoods for Airline and Disaster on the test set after finetuning each model on ten subsets of few-shot training data (as explained before in Section 5) in Figure 6 to assess whether DeepSLP exhibits this property of ensemble methods. We find that $NLL(\mathbf{F}(\mathbf{x}), y)$ is much lower than $\mathbb{E}[NLL(\mathbf{f}(\mathbf{x}), y)]$, which confirms that the joint utilisation of prototypes results in better predictions than if they were to be used individually. Our experiments confirm that this is a general trend we observe across tasks. In the following sections, we investigate the reasons behind the high values observed for $\mathbb{E}[NLL(\mathbf{f}(\mathbf{x}), y)]$, and compare the jointly trained prototypes against a strong baseline, the fine-tuned BERT baseline.

10.2 Jointly utilised soft-label prototypes improve diversity

Diversity in ensemble classifications refers to the difference in the probability distribution on out-of-distribution (ood) data for classifications between

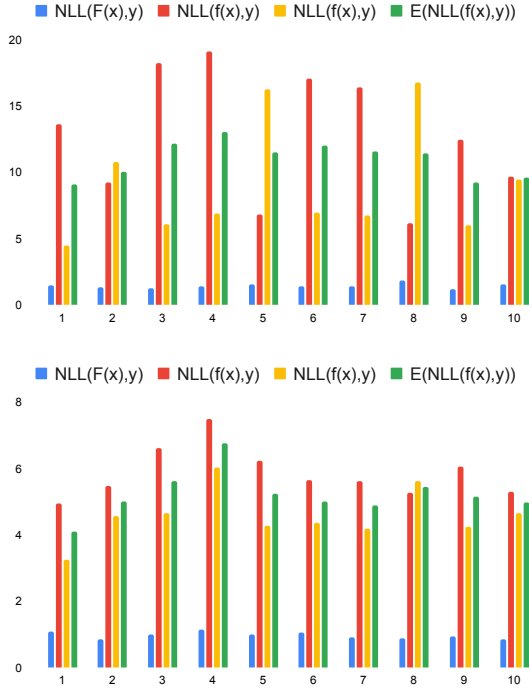


Figure 6: $NLL(\mathbf{F}(\mathbf{x}), y)$ vs. $\mathbb{E}[NLL(\mathbf{f}(\mathbf{x}), y)]$ for Disaster (top) and Airline (bottom). The i^{th} subscript refers to the i^{th} soft-label prototype.

individual models and the ensemble. We use this definition to ascertain the diversity of classifications provided by the jointly utilised soft-label prototypes. Diversity is a desirable property as ensemble predictions are generally more robust due to diversity between the predictions of their individual members (Lee et al., 2015).

Existing work (Ashukha et al., 2020; Lakshminarayanan et al., 2017) defines ensemble uncertainty as the sum of ensemble diversity and the expected average model uncertainty on ood data. Based on Abe et al. (2022), it is calculated as:

$$H([y|F(x)]) = \frac{-1}{C} \sum p(y_i|F(x)) \log(p(y_i|F(x)))$$

If we use the Jensen-Shannon divergence as a diversity measure for an ensemble given by $JSD_{p(f)}[y|f(x)] = \frac{1}{M} \sum KL[y|f(x)||y|F(x)]$ where KL is the average KL divergence between the output distribution of each soft-label prototype and the jointly utilised soft-label prototypes, from Abe et al. (2022), this expression reduces to:

$$H([y|F(x)]) = \overset{\text{ens. diversity}}{JSD_{p(f)}[y|f(x)]} + \overset{\text{avg. model uncert.}}{E_{p(f)}[H[y|f(x)]]}$$

We contrast ensemble uncertainty and single model uncertainty using the fine-tuned BERT

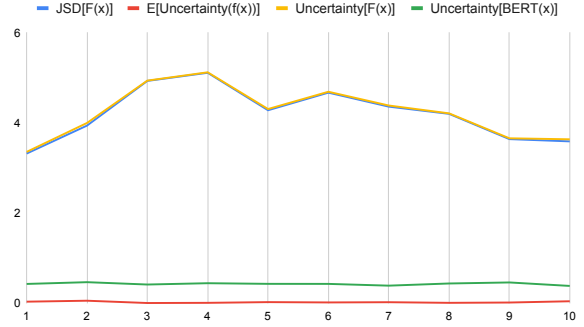


Figure 7: Ensemble uncertainty contrasted against the uncertainty of fine-tuned BERT, where we observe that DeepSLP’s uncertainty $F(x)$ (given by yellow) is driven by ensemble diversity, given by $JSD(F(x))$ in blue.

model for the task *airline* in Figure 7, but note that similar trends are observed across all tasks. We note that the uncertainty of jointly utilised soft-label prototypes is generally higher than that of the fine-tuned BERT model. As the average model uncertainty of individual soft-label prototypes is negligibly low, the uncertainty in the joint case is driven mainly by the diversity of the ensemble. This is in line with previous work which attributes an increase in uncertainty in ensembles due to diversity (Lakshminarayanan et al., 2017; Dietterich, 2000; Wilson and Izmailov, 2020). Though not strictly an ensemble, our approach exhibits similar properties (higher uncertainty driven by model diversity), as well as a general reduction in standard deviation compared to fine-tuned BERT.

The above provide evidence that our approach as a whole exhibits desirable properties of ensembles which drive a higher performance but which do not lead to a higher training time nor compute.

11 Conclusion

We developed a novel few-shot learning approach for data lean settings that is based on soft-label prototypes capturing the simultaneous membership of data points over several classes. We presented two variants, one that generates fixed prototypes via solving for linear constraints, and another that learns and generates them dynamically within a neural gradient-based optimisation approach. We evaluated our methods on 48 different tasks / settings and experimentally demonstrated that our neural approach outperforms a range of strong baselines. Finally, we presented an in-depth

analysis of the characteristics of our approach and analysed the reasons behind its effectiveness.

References

- Taiga Abe, Estefany Kelly Buchanan, Geoff Pleiss, Richard Zemel, and John P Cunningham. 2022. [Deep ensembles work, but are they necessary?](#) In *Advances in Neural Information Processing Systems*, volume 35, pages 33646–33660. Curran Associates, Inc.
- Antreas Antoniou, Harrison Edwards, and Amos Storkey. 2019. [How to train your MAML](#). In *International Conference on Learning Representations*.
- Arsenii Ashukha, Alexander Lyzhov, Dmitry Molchanov, and Dmitry Vetrov. 2020. Pitfalls of in-domain uncertainty estimation and ensembling in deep learning. *arXiv preprint arXiv:2002.06470*.
- Trapit Bansal, Rishikesh Jha, and Andrew McCallum. 2019. [Learning to few-shot learn across diverse natural language classification tasks](#).
- Trapit Bansal, Rishikesh Jha, Tsendsuren Munkhdalai, and Andrew McCallum. 2020. [Self-supervised meta-learning for few-shot natural language classification tasks](#).
- John Blitzer, Mark Dredze, and Fernando Pereira. 2007. [Biographies, Bollywood, boom-boxes and blenders: Domain adaptation for sentiment classification](#). In *Proceedings of the 45th Annual Meeting of the Association of Computational Linguistics*, pages 440–447, Prague, Czech Republic. Association for Computational Linguistics.
- Tom B. Brown, Benjamin Mann, Nick Ryder, Melanie Subbiah, Jared Kaplan, Prafulla Dhariwal, Arvind Neelakantan, Pranav Shyam, Girish Sastry, Amanda Askell, Sandhini Agarwal, Ariel Herbert-Voss, Gretchen Krueger, Tom Henighan, Rewon Child, Aditya Ramesh, Daniel M. Ziegler, Jeffrey Wu, Clemens Winter, Christopher Hesse, Mark Chen, Eric Sigler, Mateusz Litwin, Scott Gray, Benjamin Chess, Jack Clark, Christopher Berner, Sam McCandlish, Alec Radford, Ilya Sutskever, and Dario Amodei. 2020. [Language models are few-shot learners](#).
- Jiaao Chen, Zichao Yang, and Diyi Yang. 2020. [Mixtext: Linguistically-informed interpolation of hidden space for semi-supervised text classification](#).
- Kevin Clark, Minh-Thang Luong, Christopher D. Manning, and Quoc V. Le. 2018. [Semi-supervised sequence modeling with cross-view training](#).
- Jacob Devlin, Ming-Wei Chang, Kenton Lee, and Kristina Toutanova. 2018. [Bert: Pre-training of deep bidirectional transformers for language understanding](#).
- Steven Diamond and Stephen Boyd. 2016. CVXPY: A Python-embedded modeling language for convex optimization. *Journal of Machine Learning Research*, 17(83):1–5.
- Thomas G. Dietterich. 2000. Ensemble methods in machine learning. In *Multiple Classifier Systems*, pages 1–15, Berlin, Heidelberg. Springer Berlin Heidelberg.
- Zi-Yi Dou, Keyi Yu, and Antonios Anastasopoulos. 2019. [Investigating meta-learning algorithms for low-resource natural language understanding tasks](#). In *Proceedings of the 2019 Conference on Empirical Methods in Natural Language Processing and the 9th International Joint Conference on Natural Language Processing (EMNLP-IJCNLP)*, pages 1192–1197, Hong Kong, China. Association for Computational Linguistics.
- Chelsea Finn, Pieter Abbeel, and Sergey Levine. 2017. [Model-agnostic meta-learning for fast adaptation of deep networks](#).
- Tianyu Gao, Adam Fisch, and Danqi Chen. 2020. [Making pre-trained language models better few-shot learners](#).
- Xavier Glorot and Yoshua Bengio. 2010. [Understanding the difficulty of training deep feed-forward neural networks](#). In *Proceedings of the Thirteenth International Conference on Artificial Intelligence and Statistics*, volume 9 of *Proceedings of Machine Learning Research*, pages 249–256, Chia Laguna Resort, Sardinia, Italy. PMLR.
- Niels van der Heijden, Helen Yannakoudakis, Pushkar Mishra, and Ekaterina Shutova. 2021.

- Multilingual and cross-lingual document classification: A meta-learning approach. In *Proceedings of the 16th Conference of the European Chapter of the Association for Computational Linguistics: Main Volume*, pages 1966–1976, Online. Association for Computational Linguistics.
- Nithin Holla, Pushkar Mishra, Helen Yannakoudakis, and Ekaterina Shutova. 2020. [Learning to learn to disambiguate: Meta-learning for few-shot word sense disambiguation](#).
- Tushar Khot, Ashish Sabharwal, and Peter Clark. 2018. [Scitail: A textual entailment dataset from science question answering](#). In *AAAI*.
- Brenden M. Lake, Ruslan Salakhutdinov, and Joshua B. Tenenbaum. 2015. [Human-level concept learning through probabilistic program induction](#). *Science*, 350(6266):1332–1338.
- Balaji Lakshminarayanan, Alexander Pritzel, and Charles Blundell. 2017. [Simple and scalable predictive uncertainty estimation using deep ensembles](#). In *Advances in Neural Information Processing Systems*, volume 30. Curran Associates, Inc.
- Anna Langedijk, Verna Dankers, Phillip Lippe, Sander Bos, Bryan Cardenas Guevara, Helen Yannakoudakis, and Ekaterina Shutova. 2021. [Meta-learning for fast cross-lingual adaptation in dependency parsing](#).
- Stefan Lee, Senthil Purushwalkam, Michael Cogswell, David Crandall, and Dhruv Batra. 2015. [Why m heads are better than one: Training a diverse ensemble of deep networks](#).
- Brian Lester, Rami Al-Rfou, and Noah Constant. 2021. [The power of scale for parameter-efficient prompt tuning](#).
- Mike Lewis, Yinhan Liu, Naman Goyal, Marjan Ghazvininejad, Abdelrahman Mohamed, Omer Levy, Ves Stoyanov, and Luke Zettlemoyer. 2019. [Bart: Denoising sequence-to-sequence pre-training for natural language generation, translation, and comprehension](#).
- Xiang Lisa Li and Percy Liang. 2021. [Prefix-tuning: Optimizing continuous prompts for generation](#).
- Jingjing Liu, Panupong Pasupat, Scott Cyphers, and Jim Glass. 2013. [Asgard: A portable architecture for multilingual dialogue systems](#). In *2013 IEEE International Conference on Acoustics, Speech and Signal Processing*, pages 8386–8390.
- Pengfei Liu, Weizhe Yuan, Jinlan Fu, Zhengbao Jiang, Hiroaki Hayashi, and Graham Neubig. 2021. [Pre-train, prompt, and predict: A systematic survey of prompting methods in natural language processing](#). *ACM Computing Surveys*, 55:1 – 35.
- Xiaodong Liu, Pengcheng He, Weizhu Chen, and Jianfeng Gao. 2019. [Multi-task deep neural networks for natural language understanding](#).
- Ilya Loshchilov and Frank Hutter. 2017. [Decoupled weight decay regularization](#).
- Takeru Miyato, Andrew M. Dai, and Ian Goodfellow. 2016. [Adversarial training methods for semi-supervised text classification](#).
- MOSEK ApS. 2019. *The MOSEK optimization toolbox for MATLAB manual. Version 9.3*.
- Farhad Nooralahzadeh, Giannis Bekoulis, Johannes Bjerva, and Isabelle Augenstein. 2020. [Zero-shot cross-lingual transfer with meta learning](#).
- Abiola Obamuyide and Andreas Vlachos. 2019a. [Meta-learning improves lifelong relation extraction](#). In *Proceedings of the 4th Workshop on Representation Learning for NLP (RepL4NLP-2019)*, pages 224–229, Florence, Italy. Association for Computational Linguistics.
- Abiola Obamuyide and Andreas Vlachos. 2019b. [Model-agnostic meta-learning for relation classification with limited supervision](#). In *Proceedings of the 57th Annual Meeting of the Association for Computational Linguistics*, pages 5873–5879, Florence, Italy. Association for Computational Linguistics.
- Alec Radford, Jeff Wu, Rewon Child, David Luan, Dario Amodei, and Ilya Sutskever. 2019. [Language models are unsupervised multitask learners](#).
- Erik F. Tjong Kim Sang and Fien De Meulder. 2003. [Introduction to the conll-2003](#)

- shared task: Language-independent named entity recognition.
- Victor Sanh, Albert Webson, Colin Raffel, Stephen H. Bach, Lintang Sutawika, Zaid Alyafeai, Antoine Chaffin, Arnaud Stiegler, Teven Le Scao, Arun Raja, Manan Dey, M Saiful Bari, Canwen Xu, Urmish Thakker, Shanya Sharma Sharma, Eliza Szczechla, Taewoon Kim, Gunjan Chhablani, Nihal Nayak, Debajyoti Datta, Jonathan Chang, Mike Tian-Jian Jiang, Han Wang, Matteo Manica, Sheng Shen, Zheng Xin Yong, Harshit Pandey, Rachel Bawden, Thomas Wang, Trishala Neeraj, Jos Rozen, Abheesht Sharma, Andrea Santilli, Thibault Fevry, Jason Alan Fries, Ryan Teehan, Tali Bers, Stella Biderman, Leo Gao, Thomas Wolf, and Alexander M. Rush. 2021. [Multitask prompted training enables zero-shot task generalization](#).
- Timo Schick and Hinrich Schütze. 2020. [It’s not just size that matters: Small language models are also few-shot learners](#).
- Jake Snell, Kevin Swersky, and Richard S. Zemel. 2017. [Prototypical networks for few-shot learning](#).
- Ilya Sucholutsky, Nam-Hwui Kim, Ryan P. Browne, and Matthias Schonlau. 2021. [One line to rule them all: Generating LO-shot soft-label prototypes](#). In *2021 International Joint Conference on Neural Networks (IJCNN)*. IEEE.
- Ilya Sucholutsky and Matthias Schonlau. 2021. [‘less than one’-shot learning: Learning \$n\$ classes from \$m < n\$ samples](#). *Proceedings of the AAAI Conference on Artificial Intelligence*, 35(11):9739–9746.
- Chi Sun, Xipeng Qiu, Yige Xu, and Xuanjing Huang. 2020. [How to fine-tune bert for text classification?](#)
- Alex Wang, Amanpreet Singh, Julian Michael, Felix Hill, Omer Levy, and Samuel Bowman. 2018. [GLUE: A multi-task benchmark and analysis platform for natural language understanding](#). In *Proceedings of the 2018 EMNLP Workshop BlackboxNLP: Analyzing and Interpreting Neural Networks for NLP*, pages 353–355, Brussels, Belgium. Association for Computational Linguistics.
- Zirui Wang, Zachary C. Lipton, and Yulia Tsvetkov. 2020. [On negative interference in multilingual models: Findings and a meta-learning treatment](#). In *Proceedings of the 2020 Conference on Empirical Methods in Natural Language Processing (EMNLP)*, pages 4438–4450, Online. Association for Computational Linguistics.
- Andrew G Wilson and Pavel Izmailov. 2020. [Bayesian deep learning and a probabilistic perspective of generalization](#). In *Advances in Neural Information Processing Systems*, volume 33, pages 4697–4708. Curran Associates, Inc.
- Thomas Wolf, Lysandre Debut, Victor Sanh, Julien Chaumond, Clement Delangue, Anthony Moi, Pierric Cistac, Tim Rault, Rémi Louf, Morgan Funtowicz, Joe Davison, Sam Shleifer, Patrick von Platen, Clara Ma, Yacine Jernite, Julien Plu, Canwen Xu, Teven Le Scao, Sylvain Gugger, Mariama Drame, Quentin Lhoest, and Alexander M. Rush. 2019. [Huggingface’s transformers: State-of-the-art natural language processing](#).
- Qizhe Xie, Zihang Dai, Eduard Hovy, Minh-Thang Luong, and Quoc V. Le. 2019. [Unsupervised data augmentation for consistency training](#).
- Yichu Zhou and Vivek Srikumar. 2022. [A closer look at how fine-tuning changes BERT](#). In *Proceedings of the 60th Annual Meeting of the Association for Computational Linguistics (Volume 1: Long Papers)*, pages 1046–1061, Dublin, Ireland. Association for Computational Linguistics.

12 Appendix

Theorem 12.1. *SLP does not always select the nearest class centroid to a test point when using Euclidean distance.*

Consider a line l connecting three class centroids (while we focus on a three class system, the conclusions generalise to $n > 3$ classes too). The class centroids are represented by A, B and C. The soft-label prototypes at ends A and C contain the values $[a_1, a_2, a_3]$ and $[c_1, c_2, c_3]$ respectively. Consider a support example $x \in A$ at a distance d_a and d_b from A and C respectively. Directly using the constraints in Algorithm 4 of [Sucholutsky et al. \(2021\)](#), we state that the influence of A (i.e.,

the distance-weighted sum of the soft-labels at x) should be more than the sum of the influence of the other two classes. Thus, we need to maximise:

$$\frac{a_1}{d_a} + \frac{c_1}{d_b} > \left(\frac{a_2}{d_a} + \frac{c_2}{d_b} \right) + \left(\frac{a_3}{d_a} + \frac{c_3}{d_b} \right) \quad (2)$$

As we move x further towards A, $d_a \rightarrow 0$ and the influence of $[a_1, a_2, a_3]$ increases thus $\sum_{i=2}^{i=3} c_i/d_b \ll \ll \sum_{i=2}^{i=3} a_i/d_a$. Therefore we have:

$$\frac{a_1}{d_a} > \frac{a_2}{d_a} + \frac{a_3}{d_a} \implies a_1 > a_2 + a_3 \quad (3)$$

If we take a support example $x \in C$, by symmetry as x is moved towards C, $d_b \rightarrow 0$, we can also write:

$$\frac{c_3}{d_b} > \frac{c_2}{d_b} + \frac{c_1}{d_b} \implies c_3 > c_2 + c_1 \quad (4)$$

Furthermore, consider a point x in the middle of l equidistant from A and C (by a distance d) – such a point will always be classified as $x \in B$. Thus, the influence of B should be higher than both A and C. Thus we have:

$$\begin{aligned} \frac{a_2}{d} + \frac{c_2}{d} > \frac{a_1}{d} + \frac{c_1}{d} \quad \& \quad \frac{a_2}{d} + \frac{c_2}{d} > \frac{a_3}{d} + \frac{c_3}{d} \\ \implies a_2 + c_2 > a_1 + c_1 \quad \& \quad a_2 + c_2 > a_3 + c_3 \end{aligned}$$

From Equation 3 and Equation 4 we can replace a_1 and c_3 and get:

$$\begin{aligned} a_2 + c_2 > a_2 + a_3 + c_1 &\implies c_2 > c_1 \\ a_2 + c_2 > a_3 + c_2 + c_1 &\implies a_2 > a_3 \end{aligned}$$

Therefore, we have:

$$a_1 > a_2 > a_3 \quad \& \quad c_3 > c_2 > c_1$$

This is an intuitive result as the soft-label value of each class decreases as the distance of the class centroid increases from the prototype location – the class nearest to the prototype has the highest soft-label value and the class furthest away has the lowest soft-label value. Recall that $\sum_{i=1}^3 a_i = 1$ and $\sum_{i=1}^3 c_i = 1$ and $a_i, c_i \geq 0 \forall i = \{1, 2, 3\}$ otherwise the optimisation problem becomes unbounded. Therefore, the ranges of values for $[a_1, a_2, a_3]$ and $[c_1, c_2, c_3]$ are:

$$\begin{aligned} a_3 &\in [0, a_2), \quad a_2 \in (a_3, a_1), \quad a_1 \in (a_2, 1] \\ c_3 &\in (c_2, 1], \quad c_2 \in (c_1, c_3), \quad c_1 \in [0, c_2) \end{aligned}$$

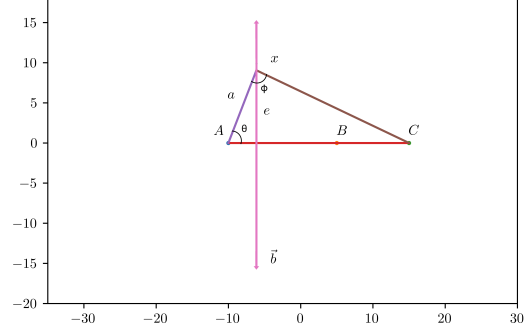


Figure 8: Schematic diagram for ascertaining θ with class centroids $A = (-10, 0)$, $B = (5, 0)$ and $C = (15, 0)$.

Using Algorithm 4 in Sucholutsky et al. (2021), we see that there are multiple constraints for a_1 and a_2 which require them to be maximised, but there are none for a_3 . Thus, to maximise Equation 3, a_3 adjusts to the minimum value it can get:

$$a_3 = \min(0, a_2) = \epsilon \simeq 0$$

By symmetry, we can also conclude that:

$$c_1 = \min(0, c_2) = \epsilon \simeq 0$$

These findings are substantiated experimentally in Table 2 – the SLP soft label corresponding to the furthest class from the prototype location drops $\simeq 0$ compared to other soft label values.

Furthermore, consider a line b perpendicular to l – it intersects l between A and B. We select θ such that $\phi = \pi/2$. We denote the complete setup diagrammatically in Figure 8.

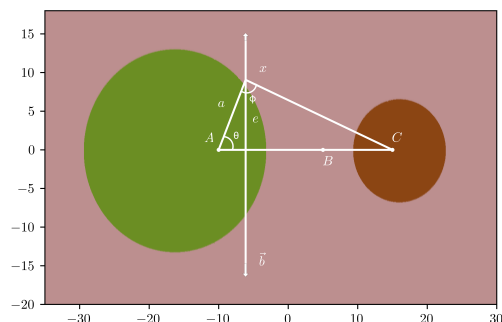
Consider the distance weighted influences at x for class A. We have the influence as $\frac{a_1 \sin \theta}{e} + \frac{c_1 \cos \theta}{e} = \frac{a_1 \sin \theta}{e}$ as $c_1 \simeq 0$. Similarly, for class B, we have the weighted influence as $\frac{a_2 \sin \theta}{e} + \frac{c_2 \cos \theta}{e}$. To calculate values of θ where the weighted influence of B is more than the weighted influence of A, we get:

$$\begin{aligned} \frac{a_2 \sin \theta}{e} + \frac{c_2 \cos \theta}{e} &> \frac{a_1 \sin \theta}{e} \\ \implies a_2 \sin \theta + c_2 \cos \theta &> a_1 \sin \theta \\ \implies c_2 \cos \theta - (a_1 - a_2) \sin \theta &> 0 \\ \implies \frac{c_2 \cos \theta - (a_1 - a_2) \sin \theta}{\sqrt{c_2^2 + (a_1 - a_2)^2}} &> 0 \\ \implies \cos(\theta + \alpha) &> 0 \end{aligned}$$

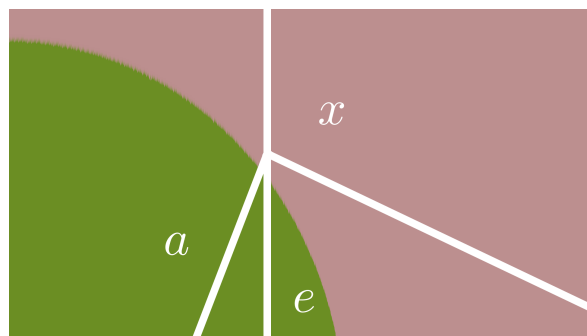
where $\alpha = \tan^{-1}\left(\frac{a_1 - a_2}{c_2}\right)$. Since $\cos(\theta + \alpha) > 0$ we have $(\theta + \alpha) \in (-\pi/2, \pi/2)$ and since $\theta > 0$, thus for $\theta \in [0, \pi/2 - \alpha)$, the weighted influence of B is more than the weighted influence of A.

However, it is worth observing the result for θ derived above can contain points closer to A (using Euclidean distance) which are *actually* classified as B. We can easily demonstrate this with a counter example explained in Figure 9.

Therefore, for points closer to A compared to B using an Euclidean measure, SLP can still return a higher value for the influence at B compared to A. This adversely affects performance in classifiers where we rely on selection of the closest class centroid for classification – such as 1-NN, Prototypical Networks, and SLP – and we believe this is the reason behind the poor performance of SLP for cases where the total number of classes is greater than two.



(a) Denoting the decision boundaries calculated with SLP. Green represents points classified as class A, pink represents the points classified as class B and brown represents the points classified as C.



(b) Zooming in at point x . We can see that it is classified as B.

Figure 9: The soft-labels of the system at A and C using SLP are calculated as $[0.5963, 0.4036, 0.0001]$ and $[0.0001, 0.4495, 0.5504]$. We also get $\theta = 66.84^\circ$. Using these soft-labels, we calculate the decision boundaries for points in this area. We use θ to calculate the coordinates of x . For x , the Euclidean distance of x from A and B is 9.847 and 14.338 respectively. From the figure, we can see that SLP classifies x as B even though the Euclidean distance of x from A is shorter.